Mesoscopic Pictures of the Sol–Gel Transition: Ladder Models and Fractal Networks

H. Schiessel* and A. Blumen

Theoretische Polymerphysik, Universität Freiburg, Rheinstrasse 12, D-79104 Freiburg, Germany

Received November 16, 1994; Revised Manuscript Received February 27, 1995®

ABSTRACT: In this work we introduce mechanical networks which highlight the relation between viscoelastic and structural properties of chemical systems at the sol–gel transition. Cross-linking polymers at the gel point show in general a power law behavior of the complex modulus, i.e., $G^*(\omega) \propto (i\omega)^\alpha$ ($0 < \alpha < 1$), which is related to the (constitutive) gel equation. We present a mechanical ladder model whose stress–strain relation obeys the gel equation with $\alpha = 1/2$ and which consists of an infinite number of springs and dashpots. Furthermore, we investigate terminated ladder arrangements which mimic pre- and postgel behavior. To elucidate the complex dependence of α on structural properties which one observes for systems near to the gel point, we analyze mechanical fractal networks.

1. Introduction

In many cases relaxation processes in complex materials show characteristic patterns; one often observes algebraic decay forms

$$\phi(t) \propto t^{-\alpha} \tag{1}$$

with $0 < \alpha < 1$ over many decades in time. Examples are current distributions at rough blocking electrodes,[1] charge-carrier transport in amorphous semiconductors,[2] the dielectric relaxation of liquids,[3] and the attenuation of seismic waves.[4]

Here we focus on the viscoelastic properties of systems of cross-linking polymers at the sol–gel transition. In typical experiments the material is exposed to a harmonic strain excitation; i.e., one measures the complex (shear) modulus $G^*(\omega)$. At the gel point this quantity often obeys a power law

$$G^*(\omega) \propto (i\omega)^\alpha \tag{2}$$

with $0 < \alpha < 1$ over many decades in frequency. This means that there is a constant phase angle between stress and strain which is independent of frequency. Using the relation $G^*(\omega) = i\omega\int_0^\infty G(\tau)\exp(-i\omega\tau)\,d\tau$, one finds for the relaxation modulus $G(t)$ (the response of the stress to a shear jump) an algebraic decay

$$G(t) \propto t^{-\alpha} \tag{3}$$

Therefore, cross-linking polymers at the sol–gel transition are very good model systems for studying algebraic decays (eq 1).

A widely used picture for the sol–gel transition is based on the percolation model which implies the appearance of critical exponents.[5] Experimentally, however, the value of α at the gel point, α_0, varies from material to material, mostly in the range from 0.2 to 0.7 (see ref 6 for an overview); this fact speaks against a universal background for α_0. We note, however, that special values for α_0 seem to be preferred, such as $\alpha_0 \cong 2/3$ and $\alpha_0 \cong 1/2$. Thus, $\alpha_0 \cong 1/2$ often appears for cross-linking polymers with balanced stoichiometry,[7,8] whereas a deficiency of the cross-linker usually leads to an increase in α_0.

The sol just below the gel point, the so-called *pregel*, shows also an ω^α behavior of the complex modulus in a bounded frequency range; for small frequencies (i.e., for large times) one finds the typical liquidlike behavior. Also the complex modulus of the system just over the gel point, the so-called *postgel*, shows (besides the typical solidlike response for small frequencies) the ω^α form. Experimentally one usually finds that α decreases monotonically during the gelation process,[7–9] so that $\alpha > \alpha_0$ for the pregel and $\alpha < \alpha_0$ for the postgel. Therefore, one has a complex dependence of α on the chemical constituents and their stoichiometry, as well as on the stage of the gelation process.

Chambon and Winter[7] proposed a rheological constitutive equation for the critical gel. In the context of the so-called fractional calculus[10,11] this equation can be interpreted as a fractional relaxation equation.[9] In this spirit Friedrich and Heymann extended in ref 9 this equation to describe the stress–strain relationship of the whole gelation process. We note that in recent years fractional calculus has become an important tool in the analysis of viscoelastic materials.[12–16] The approach is, however, rather formal and does not relate to the underlying physics at the microscopic level.

In previous works[17,18] we have developed mechanical models which can mimic fractional relaxation equations (cf. also the mechanical arrangements proposed by Heymans and Bauwens[16]). We note that ladder models, following the pioneering work of Blizard,[19] were much used as microscopic pictures for gels. Here we show that the infinite ladder model of ref 17 provides a mesoscopic description of the critical gel, whereas finite ladder systems allow one to model different gelation stages. Common to all these ladder arrangements is that they show an ω^α behavior with $\alpha = 1/2$. Furthermore, using fractal networks we provide a qualitative picture of the dependence of α on structural properties of the system, by explaining the observed decrease of α in the postgel regime.

2. Experimental Findings and Phenomenological Approaches

The mechanical properties of the gelation process have been investigated for a great variety of physical systems (see ref 6 and references therein). Here we focus on end-linking reactions where the prepolymer is far below the entanglement limit. Oscillatory shear

® Abstract published in *Advance ACS Abstracts,* April 15, 1995.

0024-9297/95/2228-4013$09.00/0

experiments of such systems show that the complex moduli at the gel point exhibit a constant phase angle behavior (cf. eq 2). An interesting problem concerns the dependence of the exponent α_0 on different physical and chemical parameters. An important class of gels are systems for which the chemical species (the prepolymers and the cross-linkers) are stoichiometrically balanced. Here one often finds $\alpha_0 \cong 1/2$, this value being rather insensitive to the choice of the prepolymers (poly(dimethylsiloxane)[7] or polyurethane[8]), to the functionality f of the cross-linker (tetrasilane, $f = 4$;[7] or triisocyanate, $f = 3$[8]), and to the chain length.[8] On the other hand, α_0 changes drastically, when the system is stoichiometrically imbalanced; i.e., α_0 increases when cross-linkers are deficient.[6-8]

Close to the gel point the complex modulus also shows an ω^α behavior in a bounded frequency range.[6-8] Thus, the pregel shows an ω^α response for $\omega \gg \omega_0$ and a typical liquidlike behavior, i.e., $G^*(\omega) \propto i\omega\tau(1 + i\omega\tau)^{-1}$, for $\omega \ll \omega_0$. For the real and imaginary parts of the complex modulus of $G^*(\omega) = G'(\omega) + iG''(\omega)$ ($G'(\omega)$ being the storage modulus and $G''(\omega)$ the loss modulus), this implies

$$G'(\omega) \propto \begin{cases} \omega^2 & \text{for } \omega \ll \omega_0 \\ \omega^\alpha & \text{for } \omega \gg \omega_0 \end{cases} \tag{4a}$$

and

$$G''(\omega) \propto \begin{cases} \omega & \text{for } \omega \ll \omega_0 \\ \omega^\alpha & \text{for } \omega \gg \omega_0 \end{cases} \tag{4b}$$

In eqs 4a and 4b ω_0 is the crossover frequency and it depends on the gelation stage of the system. With increasing cross-linking the value of ω_0 decreases toward $\omega_0 = 0$ at the gel point. Ideally, the complex modulus of the critical gel shows an ω^α behavior over the whole frequency range, i.e.

$$G'(\omega) = G''(\omega)/\tan(\alpha_0\pi/2) \propto \omega^{\alpha_0} \tag{5}$$

On the other hand, the postgel obeys an ω^α dependence for frequencies $\omega \gg \tilde{\omega}_0$ and a solidlike behavior (i.e., a nonvanishing equilibrium modulus G_∞) for $\omega \ll \tilde{\omega}_0$. Assuming that the relaxation modulus $G(t)$ reaches the equilibrium modulus G_∞ in an exponential fashion, i.e., that $G^*(\omega) - G_\infty \propto i\omega\tau(1 + i\omega\tau)^{-1}$ holds, one has for the storage and loss moduli:

$$G'(\omega) \propto \begin{cases} G_\infty & \text{for } \omega \ll \tilde{\omega}_0 \\ \omega^\alpha & \text{for } \omega \gg \tilde{\omega}_0 \end{cases} \tag{6a}$$

and

$$G''(\omega) \propto \begin{cases} \omega & \text{for } \omega \ll \tilde{\omega}_0 \\ \omega^\alpha & \text{for } \omega \gg \tilde{\omega}_0 \end{cases} \tag{6b}$$

In eqs 6a and 6b $\tilde{\omega}_0$ denotes the crossover frequency in the postgel regime; with increasing cross-linking of the system $\tilde{\omega}_0$ increases from $\tilde{\omega}_0 = 0$ at the gel point toward finite values.

As pointed out in the Introduction α depends, in general, on the gelation stage, so that, typically, for the pregel $\alpha > \alpha_0$ in eq 4 and for the postgel $\alpha < \alpha_0$ in eq 6.[7-9]

Starting from the relaxation modulus (eq 3), Chambon and Winter proposed a rheological constitutive equation for the critical gel, which they called the *gel equation*:

$$\sigma(t) = \int_{-\infty}^{t} G(t-\tau)\,\dot{\epsilon}(\tau)\,\mathrm{d}\tau = S\int_{-\infty}^{t} \frac{\dot{\epsilon}(\tau)}{(t-\tau)^\alpha}\,\mathrm{d}\tau \tag{7}$$

where $\dot{\epsilon}(t) = \mathrm{d}\epsilon(t)/\mathrm{d}t$. Equation 7 has only two material-dependent parameters, the exponent α and the gel strength S.

From the mathematical point of view, the gel expression (eq 7) is a fractional relation. To see this, we recall the *fractional integration* defined through:[10,11]

$${}_cD_t^{\gamma} f(t) = \frac{1}{\Gamma(-\gamma)}\int_c^t \frac{f(\tau)}{(t-\tau)^{1+\gamma}}\,\mathrm{d}\tau \tag{8}$$

valid for arbitrary $\gamma < 0$. The gel equation (eq 7) corresponds to having as lower limit $-\infty$ in eq 8, which is then the so-called *Weyl integral*.[10,11] In fractional rheological constitutive equations[12-17] one often uses the *Riemann–Liouville (RL) integral*, for which $c = 0$ in eq 8. RL is adequate for studying the transient material behavior after a sudden switch of the perturbation, i.e., a situation which starts from equilibrium, say having $\sigma(t) \equiv \epsilon(t) = 0$ for $t < 0$. Since we discuss here the response to harmonic excitations, the Weyl calculus is appropriate, and restricing ourselves to it, we use the symbolic notation $\mathrm{d}^\gamma/\mathrm{d}t^\gamma = {}_{-\infty}D_t^{\gamma}$. For negative, integer γ, $\gamma = -1, -2, -3, \ldots$. Equation 8 represents a multiple integral of order γ, as is readily seen by induction;[11] eq 8 can be first used to interpolate between integer, negative γ values and then to extrapolate to the positive γ-range; see refs 10 and 11 for details. One can now identify the gel equation with the following *fractional equation*:

$$\sigma(t) = S\Gamma(1-\alpha)\frac{\mathrm{d}^{\alpha-1}\dot{\epsilon}(t)}{\mathrm{d}t^{\alpha-1}} = S\Gamma(1-\alpha)\frac{\mathrm{d}^\alpha\epsilon(t)}{\mathrm{d}t^\alpha} \tag{9}$$

as introduced by Friedrich and Heymann.[9] On the right-hand side of eq 9 the composition rule for the *fractional derivative* $\mathrm{d}^\alpha/\mathrm{d}t^\alpha$ was used (see again ref 11 for the mathematical details).

To get from eq 9 the stress response to a harmonic strain excitation $\epsilon(t) \propto \exp(i\omega t)$, one has to know the fractional derivative of the exponential function. It can be shown[10,11] that

$$\frac{\mathrm{d}^\alpha \exp(i\omega t)}{\mathrm{d}t^\alpha} = (i\omega)^\alpha \exp(i\omega t) \tag{10}$$

holds for $-1 < \alpha < 1$. Hence, eq 9 is the proper constitutive equation for a material having a complex modulus of power law form (eq 2).

3. Ladder Models

Phenomenological approaches have the disadvantage that they are not directly related to the underlying physical situation. For instance (as we pointed out in ref 18), both parallel and sequential relaxation processes may result in algebraic decay patterns (eq 1). In this section we show that ladder structures allow one to describe the relaxation patterns found during the sol–gel transition.

In Figure 1 we display mechanical arrangements which lead to algebraic relaxation forms. The models

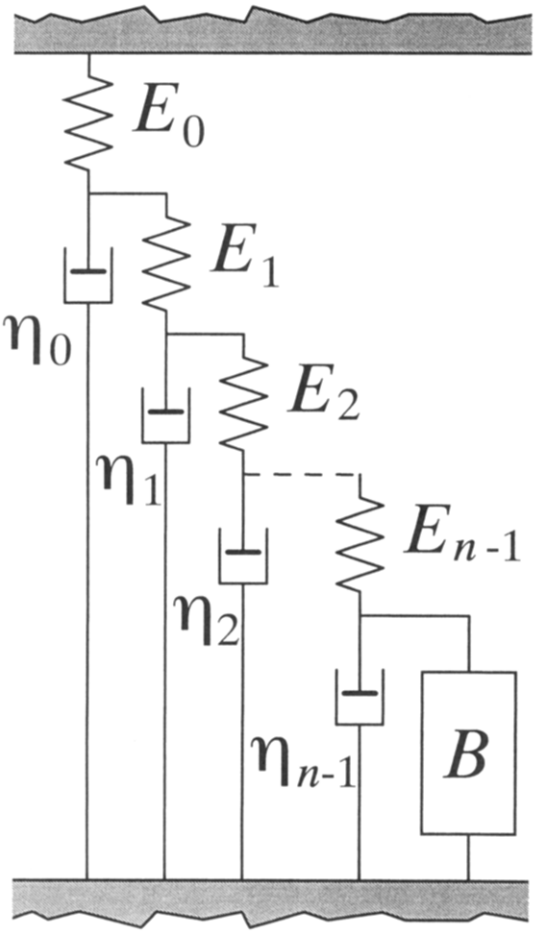

Figure 1. Ladder arrangements used to model scaling behaviors. According to the physical regime, the box B represents (a) a Maxwell element (pregel), (b) an infinite ladder (critical gel), and (c) a spring (postgel).

consist of ladderlike structures with springs (having spring constants E_0, E_1, E_2, ...) along one of the struts and dashpots (with viscosities η_0, η_1, η_2, ...) on the rungs of the ladder. Here we examine three different forms of ladder models: (a) a finite ladder structure, obtained by replacing in Figure 1 the box B by a spring E_n and a dashpot η_n in series (a so-called Maxwell element (E_n,η_n)), (b) an infinite arrangement, in which case the box B in Figure 1 represents a nonterminating ladder, and (c) a finite ladder structure, obtained by using a spring as the final rung (here the box B consists simply in a spring E_n).

Let us concentrate on the evaluation of the complex modulus. Similar to eq 32 in ref 17 (where we have evaluated $E_0\epsilon(\omega)/\sigma(\omega) = E_0/G^*(\omega)$ for the spring-terminated ladder), we obtain continued fraction expressions. The complex modulus of the infinite ladder, case b, fulfills

$$G^*(\omega) = \cfrac{E_0}{1+}\,\cfrac{(i\omega)^{-1}\frac{E_0}{\eta_0}}{1+}\,\cfrac{(i\omega)^{-1}\frac{E_1}{\eta_0}}{1+}\,\cfrac{(i\omega)^{-1}\frac{E_1}{\eta_1}}{1+}\cdots \quad (11)$$

where we use a standard notation for continued fractions, $a/(b+)\,f = a/(b+f)$, i.e., ref 20. The finite arrangements lead to terminating continued fractions. In case a we obtain

$$G^*(\omega) = \cfrac{E_0}{1+}\,\cfrac{(i\omega)^{-1}\frac{E_0}{\eta_0}}{1+}\,\cfrac{(i\omega)^{-1}\frac{E_1}{\eta_0}}{1+}\cdots\,\cfrac{(i\omega)^{-1}\frac{E_n}{\eta_{n-1}}}{1+}\,\cfrac{(i\omega)^{-1}\frac{E_n}{\eta_n}}{1} \quad (12)$$

and for case c we have

$$G^*(\omega) = \cfrac{E_0}{1+}\,\cfrac{(i\omega)^{-1}\frac{E_0}{\eta_0}}{1+}\,\cfrac{(i\omega)^{-1}\frac{E_1}{\eta_0}}{1+}\cdots\,\cfrac{(i\omega)^{-1}\frac{E_{n-1}}{\eta_{n-1}}}{1+}\,\cfrac{(i\omega)^{-1}\frac{E_n}{\eta_{n-1}}}{1} \quad (13)$$

Setting in eq 11 $E_0 = E_1 = ... = E$ and $\eta_0 = \eta_1 = ... = \eta$, it can be shown (by comparing terminating approximations of the continued fraction (eq 11) with the binomial series) that the complex modulus of the infinite arrangement is given by

$$G^*(\omega) = E\frac{(4(i\omega\tau)^{-1}+1)^{1/2}-1}{2(i\omega\tau)^{-1}} \quad (14)$$

where we set $\tau = \eta/E$. For $\omega\tau \ll 1$ eq 14 reduces to the form $G^*(\omega) \cong E(i\omega\tau)^{1/2}$. Therefore, choosing the same spring constants and viscosities for the whole arrangement, one gets a complex modulus with $\alpha = 1/2$. The short-time behavior (i.e., $\omega\tau \gg 1$) is dominated by the first spring of the ladder; in this range one obtains using eq 14 $G'(\omega) \cong E$ for the storage modulus and $G''(\omega) \cong E(\omega\tau)^{-1}$ for the loss modulus. Real materials (in general) show such a solidlike, glassy behavior, but in the measurements mentioned above[6-8] the required frequencies are out of the experimental range.

The finite arrangements a and c show fluid- and solidlike long-time behavior, respectively. To render these features of the ladder models clear, we plot in Figure 2 the frequency dependences of the storage modulus G' and the loss modulus G''; shown are case a in Figure 2a, case b in Figure 2b, and case c in Figure 2c. In all cases we set $\eta = E = 1$; for the finite arrangements we choose $n = 10^3$. In the figures one can clearly distinguish three regimes: a $\omega^{1/2}$ behavior at an intermediate frequency regime which crosses over at $\omega\tau \approx 1$ to a solidlike glassy behavior for high frequencies, whereas at low frequencies one has either a fluid- or a solidlike behavior, respectively. The crossover frequency is numerically found to be $\omega\tau \approx 4/n^2$. We hence relate case a to the pregel and case c to the postgel situation.

The long-time behavior of the finite arrangement can be derived directly from the low-frequency behavior of the complex moduli given in eqs 12 and 13 or inferred from Figure 1. We find for case a $G^*(\omega) \cong i\omega(n+1)\eta$ for $\omega\tau \ll 1$, i.e., a steady-flow viscosity $\eta_f = (n+1)\eta$. This is due to the $n+1$ dashpots in parallel terminating the arrangement. In the spring-terminated case c we find from eq 13 $G^*(\omega) \cong (n+1)^{-1}E$, i.e., an equilibrium modulus $G_\infty = (n+1)^{-1}E$. This nonvanishing value G_∞ stems from the $n+1$ springs in series connecting the upper and lower ends of the ladder. The complex moduli of finite ladder models consisting of identical springs and dashpots were also derived by Tschoegl in an alternative way.[21] We have checked numerically that his results (eq 5.2-94 of ref 21 for the pregel and eq 5.2-89 for the postgel) coincide with our continued fraction expressions.

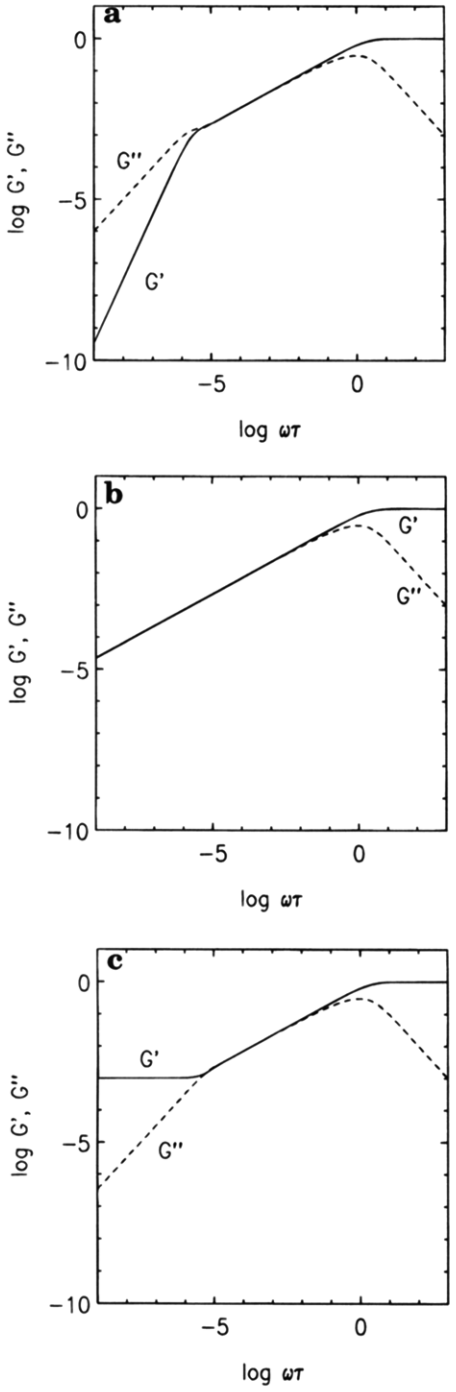

Figure 2. Storage (full line) and loss modulus (dashed line) for the a–c models of Figure 1. In all cases we set $E = \eta = 1$; for a and c we took $n = 10^3$.

To mimic closely the experimental situation, where one investigates the response of gels to a shear load, we present in Figure 3 mechanical analogues of the models shown in Figure 1, by replacing every coil spring by a horizontal series of leaf springs and the dashpots by horizontal inelastic blocks which connect all springs of one series with the next stage. The blocks are exposed to a viscous damping proportional to their velocity; this accounts for the interaction of the network with its environment. In the pregel case we have finite clusters which we take into consideration by terminating the ladder by a block (cf. Figure 3a). The infinite ladder shown in Figure 3b reflects the infinite network of the critical gel. In the postgel case the network has an excess of cross-links which leads to an elastic

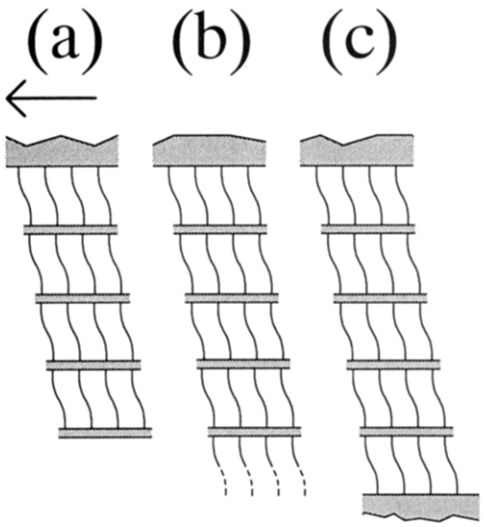

Figure 3. Mechanical analogues of Figure 1, with $n = 3$ for a and $n = 4$ for c. The arrow indicates an external shear load.

structure; for this case we terminate the system by a series of leaf springs which are connected to the bottom plate (cf. Figure 3c).

A power law of $\alpha = 1/2$ is also evident from the pioneering work of Blizard.[19] In his model the ladder structures are microscopic representations for the elastic chains, where the interactions with the surrounding medium are mediated through dashpots. His model involves then a complex averaging procedure which takes the gel fraction into account; this, however, does not affect the value of α.

So far we have discussed the case $\alpha = 1/2$. As mentioned above, this value occurs often in stoichiometrically balanced systems below the entanglement limit, whereas an imbalance in the chemical species may lead to other α values. In ref 17 we have shown how to modify the ladder model so that α takes arbitrary values between 0 and 1. For this it suffices to let the spring constants and viscosities obey

$$E_k = C_1 k^{1-2\alpha} \quad \text{and} \quad \eta_k = C_2 k^{1-2\alpha} \tag{15}$$

Inserting these values into eq 11, one can show that the continued fraction expression and therefore the complex modulus have an ω^α behavior.[17] Especially, the case $\alpha > 1/2$, which is often observed in stoichiometrically imbalanced systems, corresponds to a decrease of the spring constants and viscosities along the ladder. However, the algebraic form of the spring constants and viscosities (cf. eq 15) is rather arbitrary and is not directly related to the microscopic situation.

The dependence of the parameter α on the gelation stage and on stoichiometry lets us surmise that α reflects structural properties of the system, and here especially the connectivity of the network. A network forms differently when the number of cross-linkers varies, and the gelation process is, of course, directly related to the establishment of the topological structure. It is hence obvious that the ladder arrangements (with equal spring constants and viscosities) do not account for this fact, since they have all the same sequential connectivity; they thus lead to $\alpha = 1/2$, and the variation of n (i.e., the length of the ladder) only affects the crossover frequency ω_0.

To give a qualitative interpretation of the dependence of α on cross-linkings, we have to examine mechanical arrangements with other connectivities. In the next

section we show that fractal networks lead to an ω^α behavior with smaller values of α than in the ladder case. This highlights the dependence of α on the additional cross-links formed in the postgel regime.

4. Fractal Networks

Let us consider an arbitrary mechanical network with nodes $\boldsymbol{r}_j$. Each $\boldsymbol{r}_i$ is connected to neighboring nodes $\boldsymbol{r}_j$ by equal springs with spring constant E. Furthermore, each node is linked to a planar common ground via a dashpot with a site-dependent viscosity $\eta_i = z(\boldsymbol{r}_i)\,\eta$, where $z(\boldsymbol{r}_i)$ denotes the coordination number of node $\boldsymbol{r}_i$. The node's motion is perpendicular to the ground. Due to the stresses acting on the node $\boldsymbol{r}_i$, one gets the following equation:

$$\eta_i \dot{\epsilon}_i(t) = E \sum_{j(i)} [\epsilon_j(t) - \epsilon_i(t)] \tag{16}$$

where the sum runs over all $\boldsymbol{r}_j$ that are nearest neighbors to $\boldsymbol{r}_i$ and $\epsilon_j(t)$ denotes the displacement of node $\boldsymbol{r}_j$. The stress–strain relationship of an arbitrarily chosen node $\boldsymbol{r}_0$ with its displacement $\epsilon(t) = \epsilon_0(t)$ and the stress $\sigma(t) = \sigma_0(t)$ acting on it can be described by the following convolution integral:

$$\epsilon(t) = \int_0^t \sigma(\tau)\, U(t-\tau)\, \mathrm{d}\tau \tag{17}$$

In eq 17 the retardance $U(t)$ represents the response of the origin $\boldsymbol{r}_0$ to a δ-type stress input $\sigma(t) = \delta(t)$.[21] As we proceed to show by using results from random walk theory, for fractal networks one has an algebraic relaxation behavior of $U(t)$ at larger times, i.e.

$$U(t) \propto t^{-d_s/2} \tag{18}$$

where d_s is the so-called spectral dimension.[22] Using Tauberian theorems,[23] it follows for the Fourier transform of $U(t)$, the complex compliance $J^*(\omega)$,[21] that $J^*(\omega) \propto \omega^{d_s/2-1}$ for $\omega \to 0$ as long as $d_s < 2$. Therefore, we get for the complex modulus $G^*(\omega) = 1/J^*(\omega)$ an ω^α behavior for low frequencies with

$$\alpha = 1 - d_s/2 \tag{19}$$

It is this α which asymptotically holds for the gel equation (eq 7) (or equivalently, for the fractional equation (eq 9)) in order to describe the long-time stress–strain relationship in a fractal network with spectral dimension d_s.

To establish the connection to random walk theory and therefore to derive eq 18, we first translate the mechanical formulation in the more usual electrical version, by using one of the electromechanical analogues.[21] Therefore, we identify the springs E with conductances R^{-1} and the viscosities η_i with capacities C_i, i.e., $C_i = z(\boldsymbol{r}_i)\,C$. Then the potential $U(\boldsymbol{r}_i,t)$ at site $\boldsymbol{r}_i$ corresponds to the displacement $\epsilon_i(t)$. Using Kirchhoff's equations for each node, one obtains the following equation for the node potential $U(\boldsymbol{r}_i,t)$:

$$\frac{\mathrm{d}}{\mathrm{d}t} C_i U(\boldsymbol{r}_i,t) = R^{-1} \sum_{j(i)} (U(\boldsymbol{r}_j,t) - U(\boldsymbol{r}_i,t)) \tag{20}$$

which is equivalent to eq 16.

Such an electrical network is directly related to the following random walk problem: Consider a nearest-neighbor random walk on a fractal lattice with sites $\boldsymbol{r}_i$. Starting at the origin $\boldsymbol{r}_0$ at time $t = 0$, the probability $P(\boldsymbol{r}_i,t)$ to find the walker at site $\boldsymbol{r}_i$ at time t is determined by the master equation

$$\frac{\mathrm{d}P(\boldsymbol{r}_i,t)}{\mathrm{d}t} = \sum_{j(i)} [w_{ij} P(\boldsymbol{r}_j,t) - w_{ji} P(\boldsymbol{r}_i,t)] \tag{21}$$

with initial condition $P(\boldsymbol{r}_i,0) = \delta_{\boldsymbol{r}_i,\boldsymbol{r}_0}$. The sum runs over all nearest-neighbor sites $\boldsymbol{r}_j$ of $\boldsymbol{r}_i$, and w_{ij} is the transition probability per unit time from $\boldsymbol{r}_j$ to $\boldsymbol{r}_i$, which is specified through the coordination number $z(\boldsymbol{r}_j)$ by the relation $z(\boldsymbol{r}_j)\, w_{ij} = w$ = constant (see ref 24 for details). This equation is equivalent to eq 20 if we identify $P(\boldsymbol{r}_i,t)$ with the quantity $C_i U(\boldsymbol{r}_i,t)$ (the charge on the capacitor C_i) and the transition probability w_{ij} with the time constant $(RC_j)^{-1}$. Now, from the random walk theory on fractals,[22] the probability to be at the origin $P(\boldsymbol{r}_0,t)$ at longer times obeys:

$$P(\boldsymbol{r}_0,t) \propto t^{-d_s/2} \tag{22}$$

Since $P(\boldsymbol{r}_0,t)$ corresponds to $\eta_0 \epsilon(t)$, we have shown that eq 18 holds.

We note that except for the first spring E_0, which only affects the short-time behavior of the arrangement, the infinite ladder model described in section 3 is a special case with $d_s = 1$ and corresponds to one-dimensional diffusion. For all fractal networks one has $d_s \geq 1$.[22] Hence, in such models $\alpha = 1 - d_s/2$ varies between 0 and $1/2$, the latter value being attained for linear arrangements. The role of additional cross-links is hence to decrease the exponent α.

To be more definite, we consider a special class of fractal networks, the so-called Sierpinski-type fractals,[24] embedded in a d-dimensional Euclidean space. The generator $G(b,d)$, the basic geometrical unit from which the fractal is built up iteratively, consists of a d-dimensional hypertetrahedron of side length b, which is filled with b layers of hypertetrahedrons of unit side length (see ref 24 for details). As can be shown, the fractal dimension d_f of such an object obeys $d_f = \ln a/\ln b$, with $a = \binom{b+d-1}{d}$; hence, $\lim_{b\to\infty} d_f = d$. The spectral dimension d_s may be evaluated for each Sierpinski-type fractal using the methods of ref 24. For example, for $b = 2$ one has

$$d_s = 2\ln(d+1)/\ln(d+3) \tag{23}$$

which spans the interval $1.365... \leq d_s < 2$. As shown numerically,[24] for fixed d the spectral dimension d_s increases with b and reaches asymptotically the upper limit $d_s = 2$.

In Figure 4 we show details of the infinite network for the case $b = d = 2$ which characterizes the usual Sierpinski gasket. On top we display the electrical system, in the middle the mechanical analogue, and at the bottom a version similar to Figure 3. To allow a direct comparison with the ladder model, we have arranged the structural parts in such a way that one can easily see the additional cross-links of the network which connect different parts of the (bold figured) ladder in a self-similar manner. The origin $\boldsymbol{r}_0$ is at the top of the triangle displayed, and in the mechanical version we have inserted an additional first spring.

The evolution of the system in the postgel regime can now be visualized as follows: Starting from an effectively one-dimensional situation, additional cross-links create an increasingly dense structure, correspond-

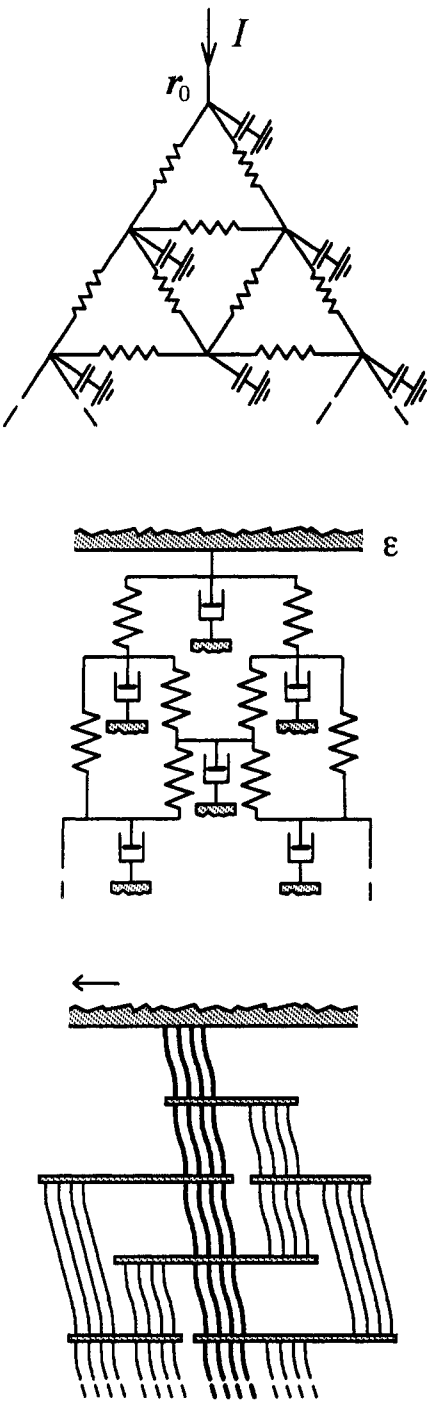

Figure 4. From the top to the bottom details of the infinite Sierpinski gasket in the electrical version and two mechanical analogues (see text for details).

ing (for a self-similar network) to an increase of the spectral dimension; this is tied to a monotonic decrease of the observed parameter α.

So far we have considered only the parameter α which characterizes the relaxation at intermediate frequencies. At low frequencies, the pregel (postgel) behaves as a liquid (solid). As in section 3, one can account for this fact by using only finite fractal patterns (by stopping the recursive construction after several steps) and by using adequate boundary conditions. Using a scaling approach, Clerc et al.[25,26] have derived the impedance of the electrical system for finite Sierpinski gaskets ($b = d = 2$). Generalizing this scaling approach to arbitrary values of b and d, we find for the complex modulus

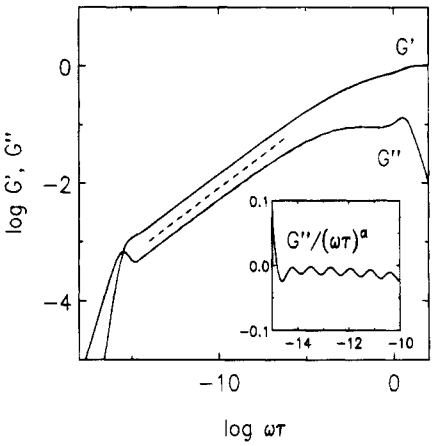

Figure 5. Storage and loss modulus of the Sierpinski network with $b = 2$ and $d = 3$ at stage $n = 20$. The inset displays a magnification of the rescaled loss modulus (see text).

of the nth generation:

$$G_n^*(\omega) \cong \begin{cases} L^{d_f}(d+1)i\omega\eta & \text{for } \omega\tau \ll L^{-d_w} \\ c(i\omega)^{\alpha} & \text{for } L^{-d_w} \ll \omega\tau \ll 1 \\ i\omega\eta & \text{for } \omega\tau \gg 1 \end{cases} \quad (24)$$

In eq 24 $\tau = \eta/E$ and $\alpha = 1 - d_s/2$. The values of α obtained here are less than $^1/_2$ (as intuitively expected for connected lattices) and can be compared to the measurements for postgel materials; c denotes either a constant or a periodic function of $\ln \omega\tau$.[25,26] However, here the oscillations are usually small, so that for practical purposes c can be viewed as being a constant. The lower crossover frequency $\omega_0 = \tau^{-1}L^{-d_w}$ depends on the size of the system $L = b^n$ and on the random-walk exponent $d_w = 2d_f/d_s$.[22] Especially, for $b = 2$ one has $\omega_0 = \tau^{-1}(d+3)^{-k}$.

As they stand, the finite arrangements considered here show fluidlike behavior, $G^* \propto \omega$, at low and high frequencies. Glassy short-time behavior can be mimicked by letting the external force act on the origin $\boldsymbol{r}_0$ via a spring E. Solidlike long-time behavior may be obtained by replacing some dashpots (for example, at the main corners) by springs which are connected to the ground. Such modifications, however, break the self-similarity of the network.

In Figure 5 we display the complex modulus of the finite Sierpinski-type network with $b = 2$, $d = 3$, and $n = 20$. Here we have taken also the additional spring E at $\boldsymbol{r}_0$ into account. To calculate $G_n^*(\omega)$ explicitly, we have used recursion formulas as given in ref 25. In Figure 5 one can distinguish three regimes: a fluidlike behavior (i.e., $G' \propto \omega^2$ and $G'' \propto \omega$) at low, an ω^{α} behavior at intermediate, and a solidlike behavior, $G' \cong E$ and $G'' \cong E(\omega\tau)^{-1}$, at high frequencies. Here $\alpha = 1 - d_s/2 = 1 - 2\ln 2/\ln 6 \cong 0.226$ (cf. eq 24); this slope is indicated in the figure by a dashed line. The solidlike behavior is due to the additional spring at $\boldsymbol{r}_0$. The crossover frequency between the fluidlike and the ω^{α} range occurs at $\omega_0\tau \cong (d+3)^{-n} = 6^{-20} \cong 2.7 \times 10^{-16}$; the crossover to the solidlike range occurs at $\omega\tau \approx 1$. The direct comparison shows a qualitatively similar behavior to the Maxwell-terminated ladder model (Figure 2a). One should note that at intermediate frequencies G' and G'' coincide in the ladder case (see eq 5 with $\alpha = {}^1/_2$), whereas in the Sierpinski case they differ by a factor $\tan(\alpha\pi/2)$. To display the small oscillations of G^* which are characteristic of deterministic fractals, we show in the inset of Figure 5 a magnification of the rescaled loss

modulus G''. Using scaling arguments, one finds for the period ln 6. This observation is consistent with numerical simulations of random walks on Sierpinski gaskets.[27] We note, however, that these oscillations reflect the deterministic hierarchical structure of the fractal investigated, whereas we do not expect this phenomenon in the usual gels.

5. Conclusion

In this work we have presented mechanical arrangements consisting of springs and dashpots which mimic the rheological properties of systems of cross-linking polymers near the gel point. Ladderlike structures lead to scaling laws for the complex (shear) modulus, usually with a power law exponent $\alpha = 1/2$. The dependence of the parameter α on the structural properties of the gel can be rendered evident by the use of models based on fractal networks. As shown, the parameter α is related to the spectral dimension d_s of the fractal and describes the postgel situation. Special aspects of the pre- and postgel behavior can be rationalized by using finite fractal patterns.

Acknowledgment. This work was supported by the SFB 60 of the DFG and by the Fonds der Chemischen Industrie.

References and Notes

(1) Bates, J. B.; Chu, Y. T. *Solid State Ionics* **1988**, *28–30*, 1388.
(2) Scher, H.; Montroll, E. W. *Phys. Rev.* **1975**, *B12*, 2455.
(3) Cole, K. S.; Cole, R. H. *J. Chem. Phys.* **1941**, *9*, 341.
(4) Kjartansson, E. *J. Geophys. Res.* **1979**, *84*, 4737.
(5) de Gennes, P.-G. *Scaling Concepts in Polymer Physics*; Cornell University Press: Ithaca, NY, 1979.
(6) Scanlan, J. C.; Winter, H. H. *Macromolecules* **1991**, *24*, 47.
(7) Chambon, F.; Winter, H. H. *J. Rheol.* **1987**, *31*, 683.
(8) Winter, H. H.; Morganelli, P.; Chambon, F. *Macromolecules* **1988**, *21*, 532.
(9) Friedrich, C.; Heymann, L. *J. Rheol.* **1988**, *32*, 235.
(10) Oldham, K. B.; Spanier, J. *The Fractional Calculus*; Academic Press: New York, London, 1974.
(11) Miller, K. S.; Ross, B. *An Introduction to the Fractional Calculus and Fractional Differential Equations*; Wiley: New York, 1993.
(12) Glöckle, W. G.; Nonnenmacher, T. F. *Macromolecules* **1991**, *24*, 6426.
(13) Glöckle, W. G.; Nonnenmacher, T. F. *Rheol. Acta* **1994**, *33*, 337.
(14) Friedrich, C.; Braun, H. *Rheol. Acta* **1992**, *31*, 309.
(15) Friedrich, C.; Braun, H. *Colloid Polym. Sci.* **1994**, *272*, 1536.
(16) Heymans, N.; Bauwens, J.-C. *Rheol. Acta* **1994**, *33*, 210.
(17) Schiessel, H.; Blumen, A. *J. Phys. A: Math. Gen.* **1993**, *26*, 5057.
(18) Schiessel, H.; Alemany, P.; Blumen, A. *Progr. Colloid Polym. Sci.* **1994**, *96*, 16.
(19) Blizard, R. B. *J. Appl. Phys.* **1951**, *22*, 730.
(20) Abramowitz, M., Stegun, I. A., Eds. *Handbook of Mathematical Functions*; Dover: New York, 1972.
(21) Tschoegl, N. W. *The Phenomenological Theory of Linear Viscoelastic Behavior*; Springer: Berlin, 1989.
(22) Havlin, S.; Bunde, A. In *Fractals and Disordered Systems*; Bunde, A., Havlin, S., Eds.; Springer: Berlin, 1991; pp 97–149.
(23) Feller, W. *An Introduction to Probability Theory and Its Applications*; Wiley: New York, 1971; Vol. II.
(24) Hilfer, R.; Blumen, A. *J. Phys. A: Math. Gen.* **1984**, *17*, L537.
(25) Clerc, J. P.; Tremblay, A.-M. S.; Albinet, G.; Mitescu, C. D. *J. Phys. Lett., Paris* **1984**, *45*, L913.
(26) Clerc, J. P.; Giraud, G.; Laugier, J. M.; Luck, J. M. *Adv. Phys.* **1990**, *39*, 191.
(27) Klafter, J.; Zumofen, G.; Blumen, A. *J. Phys. A: Math. Gen.* **1991**, *24*, 4835.

MA9461815